Numerical simulations of shot noise in degenerate disordered conductors in reduced dimensions

Andrzej Kolek, Adam Witold Stadler, and Grzegorz Hałdaś
Department of Electronics Fundamentals, Rzeszów University of Technology, Rzeszów, Wincentego Pola 2, PL 35-959, Poland
(Received 19 February 2001; published 17 July 2001)

Monte Carlo calculations of shot noise power S in one- and two-dimensional Anderson models of a disordered conductor are presented. For quasi-one-dimensional geometry all theoretical results derived from random matrix theory are confirmed in ballistic-to-diffusive, metallic, and weak localization regimes. For two dimensions in the weak localization regime the relation $S=\frac{1}{3}G+\delta\tilde{S}2e^2/h$ with $\delta\tilde{S}=0.123\,74$ is found. In the ballistic-to-metallic and strongly localized regimes both one- and two-dimensional geometries behave in the same manner.

DOI: 10.1103/PhysRevB.64.075202 PACS number(s): 71.15.Ap, 72.70.+m, 72.10.−d

I. INTRODUCTION

Shot noise in a conductor is a consequence of charge quantization. It appears everywhere where the particle is transmitted with probability that is less than 1 but more than 0. This leads to fluctuations of the current around its average value $\langle I\rangle$. A famous example is the tunnel barrier with small but finite transmission probability for which Schottky's result for shot noise holds,[1]

$$S_I(0)\equiv S_I=2e\langle I\rangle, \tag{1}$$

where S_I is the zero-frequency limit of the current noise power. This result is often referred to in the literature as the Poissonian value of shot noise.

Recently an increasing interest in shot noise in mesoscopic conductors has been observed.[2] One reason for this is that its measurements can give complementary information about the systems with respect to ordinary conductance measurements. The mentioned increasing interest refers to both the experimental and theoretical sides of the phenomenon. On theoretical grounds two main approaches are being used: the classical Langevin and Boltzmann-Langevin methods and scattering (Landauer) approach to electrical conductance. The latter which is also used in this paper has the advantage of a proper treatment of fully phase-coherent mesoscopic conductors. For a two-terminal case and a system at thermal equilibrium in the zero-temperature limit the conductance can be expressed as

$$G=\frac{2e^2}{h}\mathrm{Tr}(\mathbf{t}^{+}\mathbf{t})=\frac{2e^2}{h}\sum_n T_n, \tag{2}$$

where T_n are eigenvalues of the transmission matrix square $\mathbf{t}^{+}\mathbf{t}$. In this basis the nonequilibrium shot noise is given as[3]

$$S_I=\frac{4e^3|V|}{h}\sum_n T_n(1-T_n), \tag{3}$$

which only in the limit of small T_n's reduces to the Schottky's results of Eq. (1). It is obvious from Eqs. (1)–(3) that shot noise is always suppressed in comparison to the Poissonian limit of Eq. (1). A useful measure of this suppression is the Fano factor F which is defined as

$$F\equiv\frac{S_I}{2e\langle I\rangle}=\frac{\sum_n T_n(1-T_n)}{\sum_n T_n}. \tag{4}$$

For disordered conductors in the metallic diffusion regime the value of the Fano factor was proved to be 1/3.[4] This was confirmed experimentally by Henny *et al.*[5] The real reason for 1/3 suppression of shot noise power is that the transmission coefficients T_n have a bimodal distribution which apart from closed channels with eigenvalues $T_n\ll 1$ contains the number of open channels with $T_n\sim 1$.[6] Such a form of the distribution is well explained by random matrix theory (RMT).[7] Although this theory in principle describes one-dimensional (1D) transport, the result of 1/3 suppression of shot noise in the metallic diffusive regime holds also for higher dimensionalities[8] and thus appears as ''superuniversal.'' Similar superuniversal behavior is expected in the localized regime, where both conductance and shot noise decay exponentially with length L. As in tunnel barriers, shot noise is not suppressed: $F=1$.

It is not clear whether the suppression of shot noise in the weakly localized regime is also superuniversal. For one-dimensional geometry it was shown that quantum interference effects due to disorder lead to corrections in the shot noise power $S\equiv S_I/(2eV)$ and conductance,[9,10]

$$S=\frac{2e^2}{h}\left(\frac{N_\perp l}{3L}-\frac{1}{45}\right), \tag{5}$$

$$G=\frac{2e^2}{h}\left(\frac{N_\perp l}{L}-\frac{1}{3}\right), \tag{6}$$

where $N_\perp$ is the number of transverse channels, and l is the mean free path due to the disorder. Equations (5) and (6) yield the S vs G relation in the weakly localized regime:

$$S=\frac{1}{3}G+\frac{4}{45}\left(\frac{2e^2}{h}\right). \tag{7}$$

Although the theory of weak localization in the transmission matrix has been worked out also for two- and three-dimensional geometries,[11] to our knowledge no clear answer

whether Eq. (7) holds also in 2D and 3D has been given so far. Another still open question is the crossover from the metallic to the localized regime which for shot noise has not been investigated yet. This is contrary to the transition to the ballistic regime, which for one-dimensional geometry was found to behave as[9]

$$F=\frac{1}{3}\left(1-\frac{1}{(1+L/l)^3}\right). \tag{8}$$

In this paper we address the open questions mentioned above. Our main result is that in two dimensions Eq. (7) also holds, however with correction terms of $0.123\,74\ldots$ rather than of 4/45. We have achieved this result by means of numerical simulations and by making use of the microscopic calculations of the distribution of eigenvalues of the $\mathbf{t}^{+}\mathbf{t}$ matrix developed by Nazarov.[11] Our numerical simulations also show that for shot noise the crossover from the weakly to strongly localized regime can be described in terms of only one parameter: namely, the conductance G of the system.

This paper is organized as follows. In the next section we briefly describe the model of a disorder conductor and the method of calculation we have used. In Sec. III we present the results of calculations concerning the transition from the ballistic to the diffusive regime. Our results clearly show that Eq. (8) correctly describes this crossover not only in quasi-one-dimensional geometries but also for $d=2$. The increasing disorder drives the conductor to weak and then to strong localization. The behavior of shot noise in this regime is described in Secs. IV and V. Eventually, Sec. VI contains a brief summary and conclusions.

II. MODEL OF THE DISORDER CONDUCTOR AND METHOD OF CALCULATION

We consider the Anderson model with diagonal disorder, which is commonly used in studies of disorder conductors. It is provided by the spinless one-particle periodic tight-binding Hamiltonian

$$H=\sum_i \varepsilon_i|i\rangle\langle i|+t\sum_{i,j}|i\rangle\langle j|, \tag{9}$$

where the summation in the second term runs only over nearest neighbors (NN). Here ε_i are the energies at sites i of the lattice and t is the hopping matrix element. Disorder is introduced by taking the site energies at random and assuming a box probability distribution for them:

$$p(\varepsilon_i)=\begin{cases}\dfrac{1}{W} & \text{for } |\varepsilon_i|<W/2,\\ 0 & \text{otherwise.}\end{cases} \tag{10}$$

The distribution given by Eq. (10) was applied to all sites of rectangular disordered samples of size $w\times L$ (both in units of lattice spacing a). Two perfect leads (i.e., with $\varepsilon_i=0$) were attached to the opposite (left and right) sides of the sample. They took the shape of semi-infinite wires of width w. Hard wall boundaries for both the sample and the leads were assumed in the remaining direction. For two-dimensional conductors a square geometry with width $w=L$ was taken. To calculate the elements of the transmission matrix $\mathbf{t}$ we have used the Fisher-Lee relation which express them in terms of the Green's function[12,13]

$$[\mathbf{t}]_{mn}=\sum_{j\in L1}\sum_{k\in L2} i\chi_n(ja)\sqrt{v_n}[\mathbf{G}]_{kj}\sqrt{v_m}\chi_m(ka), \tag{11}$$

where χ_n and χ_m are transverse components of envelope functions, v_n and v_m are longitudinal velocities of incoming and outgoing waves, respectively, and the sums are over all sites in the leads $L1$ (left) and $L2$ (right) that lie on the sample-to-lead edge.

The Green's function elements that appear in Eq. (11) describe the response at sites k lying on the right edge of the conductor due to excitations at sites j that lie on the left edge. They were calculated by inverting the matrix

$$\mathbf{G}=[E\mathbf{I}-\mathbf{H}-\mathbf{\Sigma}_{L1}-\mathbf{\Sigma}_{L2}]^{-1}, \tag{12}$$

where $\mathbf{\Sigma}_{L1}$, $\mathbf{\Sigma}_{L2}$ are the self-energies due to the leads.[12] Once the transmission matrix $\mathbf{t}$ was evaluated, the eigenvalues of the matrix $\mathbf{t}^{+}\mathbf{t}$ were calculated by the standard LAPACK procedure. All calculations were performed for energy near the band center $E=0.5t$.

The calculations were performed for 10 000 configurations of the disorder potential of which the results were then averaged. The quantities being averaged were (i) the sum of eigenvalues $\langle\Sigma_n T_n\rangle$ or equivalently the conductance $\langle G\rangle$, (ii) the sum of eigenvalues squared $\langle\Sigma_n T_n^2\rangle$ which is necessary to compute the average shot noise power $\langle S\rangle=\langle\Sigma_n T_n^2\rangle-\langle\Sigma_n T_n\rangle$, and (iii) the Fano factor $\langle F\rangle$.

Apart from this real-time averaging all the results were stored in memory so that calculations of both the conductance and shot noise power rms fluctuations

$$\text{rms}\,G=\sqrt{\langle(G-\langle G\rangle)^2\rangle},\quad \text{rms}\,S=\sqrt{\langle(S-\langle S\rangle)^2\rangle} \tag{13}$$

were possible after completing every simulation run. The calculations were performed mostly as a function of lattice size L with other parameters being fixed. Such finite-size scaling was performed for several degrees of disorder starting from weak disorder with $W=1$ up to strong disorder with $W=12$.

III. BALLISTIC-TO-DIFFUSIVE CROSSOVER

As the degree of disorder is weak a conductor exhibits ballistic behavior. The word ''ballistic'' reflects the fact that in this case the mean free path l is larger than the size (length) L of the sample. All transverse modes are transmitted with probability $T\sim 1$ and this means that shot noise is suppressed [due to the factors $(1-T_n)$ in Eq. (3)]. Alternatively the Fano factor is nearly 0. As either disorder (W) or the length of the sample increases the condition $l\ll L$ holds no longer. The systems cross over to the metallic regime where the transport is diffusive and the Fano factor approaches the value $F=1/3$. In this region we have $l\ll L$. For one- and two-dimensional geometries, however, to be in the

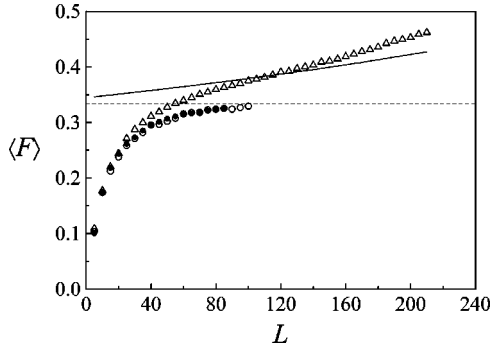

FIG. 1. Fano factor $\langle F\rangle$ versus the length L of weakly disordered conductors. Open symbols are for one-dimensional strips of width $w=10$ (triangles) or $w=100$ (circles). Solid dots are for square ($w=L$) geometry. The horizontal dashed line is at $\langle F\rangle = 1/3$. The solid line is the plot of Eq. (14). Each data point is the average of 1000 configurations. The strength of the disordered potential was $W=1$.

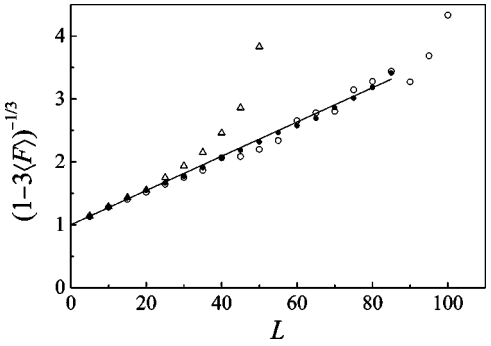

FIG. 2. Data from Fig. 1 in different coordinates. The meaning of the symbols is preserved. The solid line is the plot of Eq. (8), with $l=36.7$ (in units of a).

metallic regime the size of the system must be much smaller than the localization length $L \ll \xi_l$. Those two conditions—i.e., $l \ll L$ and $L \ll \xi_l$—impose very hard requirements on the system width. Indeed in one dimension we have $\xi_l = N_\perp l$ which means that a large number of transverse modes is necessary which (as $N_\perp \sim w$) means that a strip should be wide enough. It is hard to achieve in numerical simulations the width, say, $w>100$ and $L \gg w$, so what one could expect is a crossover from the ballistic to the weakly localized regime rather than to a purely diffusive one. This can be easily observed in Fig. 1 where finite-size scaling calculations of the Fano factor for two one-dimensional strips of different widths but the same degree of disorder $W=1$ are shown. For a wide strip the localization length is larger and the crossover is from the ballistic to the metallic regime where $F=1/3$. This is not the case for a narrow strip for which, since ξ_l is much shorter, the crossover is from the ballistic directly to the weak localization regime where Eqs. (5) and (6) yield

$$F = \frac{1}{3} + \frac{4}{45}\frac{1}{G}\left(\frac{2e^2}{h}\right). \tag{14}$$

In Fig. 1 also the results for two-dimensional lattice (with the same value of $W=1$) are shown. They coincide with one-dimensional data for a wide strip.

The ballistic-to-diffusive regime crossover was studied by de Jong and Beenakker[9] who found Eq. (8). Our numerical simulations confirm that this relation indeed describes this crossover very well. This is shown in Fig. 2 where the data from Fig. 1 are replotted in $(1-3F)^{-1/3}$ versus L coordinates. In agreement with Eq. (8) they follow a straight line which intersects the y axis at $y=1$. The slope of this line gives the mean free path $l=36.7$. Monte Carlo simulations of shot noise for the situation of the ballistic-to-diffusive crossover were performed by Liu *et al.*[14] who also found agreement with Eq. (8). What is new in our results is that data for two-dimensional $L\times L$ samples also follow Eq. (8). This means that this relation holds also for higher dimensionalities. This is not very surprising if we look at Fig. 3 where crossover trajectories for two 1D strips and a 2D square are drawn together. The 2D trajectory is composed from data which lie also on trajectories for 1D strips of various widths. The latter obey Eq. (8) so also the 2D trajectory obeys this equation provided the mean free path l is only a function of the degree of disorder and does not depend on the strip width.

IV. WEAK LOCALIZATION

In the weakly localized regime the condition $L \ll \xi_l$ does not have to be fulfilled. This makes the simulations easier. Very wide strips are not necessary. In Fig. 4 the results for 30 site wide strips of different lengths are shown. The region of weak localization where Eq. (7) should hold is clearly evident. This confirms the validity of the random matrix analysis by which this relation has been obtained.[9] To our knowledge this is the first numerical study which shows agreement with Eq. (7). In Fig. 5 results for two-dimensions are displayed. Here the data in the weak localization regime $G \gg 1$ tend to approach the line

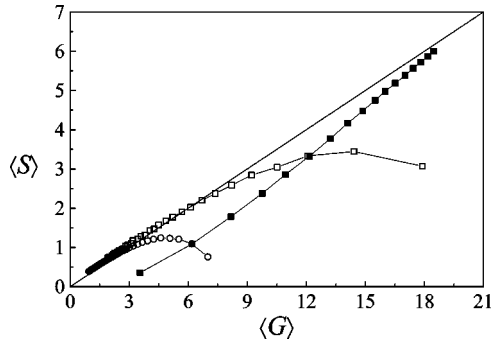

FIG. 3. Shot noise power $\langle S\rangle$ versus conductance $\langle G\rangle$ (both in units of $2e^2/h$) for $W=1$. Open symbols are for quasi-1D strips of width $w=10$ (circles) or $w=30$ (squares). Solid symbols are for square $L\times L$ (2D) geometry. The line is the plot of $S=\frac{1}{3}G$, which is the metallic diffusive limit. For the 1D case the flow of trajectories is from the right to the left (decreasing conductance) with increasing length L of the strips. For the 2D case it is just the opposite (until the diffusive limit is achieved). Data are averages over 10 000 configurations.

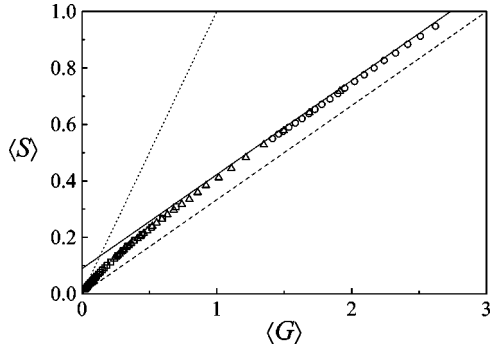

FIG. 4. Shot noise power $\langle S\rangle$ versus conductance $\langle G\rangle$ (both in units of $2e^2/h$) for a quasi-1D disorder conductor. Symbols are for various degrees of disorder $W=1$ (circles), $W=2$ (triangles), and $W=3$ (squares). The width of the conductor was $w=30$ while its length was increasing from $L=230$ up to $L=430$ ($W=1$), from $L=80$ up to 370 for $W=2$, and from $L=80$ up to 380 for $W=3$. In each case G (and S) decreases with L increasing. The solid line is the plot of Eq. (7) which is the metallic diffusive limit $S=\frac{1}{3}G$ (dashed line) corrected for weak localization. The dotted line is the (strong) localization limit $S=G$.

$$S=\frac{1}{3}G+0.1237\left(\frac{2e^2}{h}\right). \tag{15}$$

Below we prove that the difference in the factors for 1D and 2D cases, namely, 4/45 and 0.123 74 . . . , is not accidental or caused by numerical errors. To show this we employ the microscopic theory of weak localization corrections to eigenvalues of the matrix $\mathbf{t}^+\mathbf{t}$.[11] The easiest method to treat analitycally weak localization corrections to shot noise with this theory is to use relation (16) of Ref. 11 which in our case of an orthogonal ensemble reads

$$\sin\phi\,\delta F(\phi)=-2\phi\sum_s \frac{1}{s^2-\phi^2}. \tag{16}$$

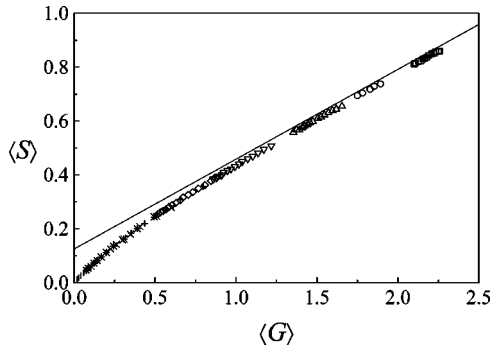

FIG. 5. Same as Fig. 4 but for two-dimensional $L\times L$ geometry. The meaning of the symbol is square for $W=3$, circle for $W=3.25$, up triangle for $W=3.6$, down triangle for $W=4$, diamond for $W=4.5$, cross (+) for $W=5$, cross (×) for $W=6$, star for $W=6.5$, and vertical bar (|) for $W=8$. The line is the plot of Eq. (15). The size L of the square-shaped samples was varied from $L=10$ (for $W\geqslant 5$), 20 (for $W=4.5$ and $W=4$, and $W=3.5$), 30 (for $W=3.25$ and $W=3$), up to $L=90$. (Data from the ballistic regime for small W's are skipped.) Averages were taken over 10 000 configurations.

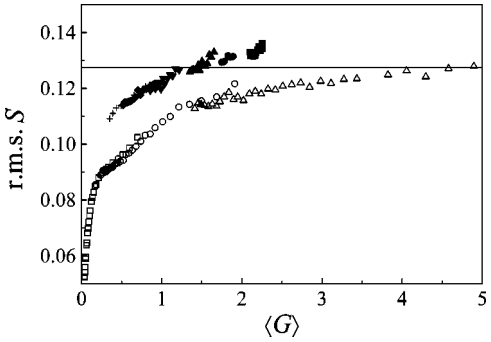

FIG. 6. rms fluctuations of shot noise power versus average conductance $\langle G\rangle$ for 1D (open symbols) and 2D (solid symbols) geometries. The meaning of the symbols is the same as in Fig. 4 for $d=1$ or in Fig. 5 for $d=2$. The horizontal line is the theoretical limit derived from RMT: rms $S=\sqrt{\frac{46}{2385}}$.

For three-dimensional cube geometry $s^2=\pi^2\Sigma_{i=x,y,z}n_i^2$ and n_i are integer numbers labeling discrete diffusion modes. If x is the direction of transport, then n_x starts from 1, whereas n_y, n_z range from 0 to infinity. By virtue of the definition of the generating function $\delta F(\phi)$ [Eq. (8) of Ref. 11], namely,

$$\delta F(\phi)=\delta\,\mathrm{Tr}\left(\frac{\mathbf{t}^+\mathbf{t}}{\mathbf{1}-\sin^2\frac{\phi}{2}\mathbf{t}^+\mathbf{t}}\right), \tag{17}$$

all the moments of the distribution of transmission eigenvalues can be expressed via derivatives of $\delta F(\phi)$ at $\phi=0$. In particular,

$$\delta\mathrm{Tr}(\mathbf{t}^+\mathbf{t})=\delta F(0),\quad \delta\mathrm{Tr}(\mathbf{t}^+\mathbf{t})^2=4\frac{d}{d\phi^2}\delta F(\phi)\big|_{\phi=0}. \tag{18}$$

From Eq. (17) one can deduce that $S=\frac{1}{3}G+\delta\tilde{S}2e^2/h$ with

$$\delta\tilde{S}=8\sum_s s^{-4}. \tag{19}$$

For the 1D case it gives $\delta\tilde{S}_{1\mathrm{D}}=(8/\pi^4)\zeta(4)=\frac{4}{45}$ whereas for 2D and 3D numerical evaluation of the above sum gives

$$\delta\tilde{S}_{2\mathrm{D}}=0.123\,74\ldots,\quad \delta\tilde{S}_{3\mathrm{D}}=0.209\ldots.$$

The value of $\delta\tilde{S}$ in 2D is in excellent agreement with our numerical simulations in Fig. 5. To our knowledge this result is quite new. It is not clear whether the values of $\delta\tilde{S}$ we have obtained in our analysis can be treated as a numerical approximation of any rational number. To answer this question one has to be able to perform analytically the summation in Eq. (19). To our knowledge this has not been done so far.

The small difference in a factor by which shot noise exceeds the metallic diffusive limit $S=\frac{1}{3}G$ is not the only effect which distinguishes one- and two-dimensional geometries. Another one is a (small) difference in rms fluctuations of shot noise power. This is shown in Fig. 6 where data for $d=1$ and $d=2$ are plotted together. For one-dimensional

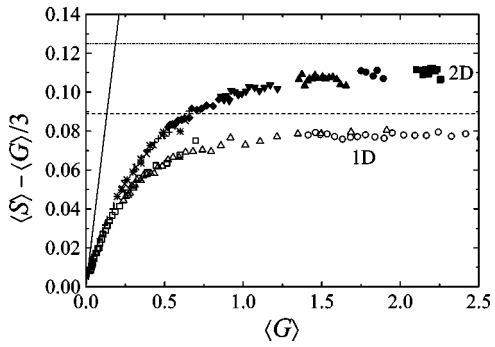

FIG. 7. Data from Figs. 4 and 5 replotted in $(S-\frac{1}{3}G)$ vs G coordinates. New data series for stronger disorder (up to $W=12$) are added. Solid and open symbols (upper and lower branches) illustrate data for 2D and 1D, respectively. Asymptotic lines are added as for reference; horizontal lines are weak localization limits for 1D (dashed) and 2D (dot-dashed) and the solid line is the strong localization limit.

geometry and for $G \gg 1$ they reach the theoretical limit of $\sqrt{43/2385}$.[9,16] This limit seems to be slightly higher for two dimensions.

V. CROSSOVER TO THE STRONGLY LOCALIZED REGIME

With increasing disorder (W) the conductor enters the strongly localized regime. In Figs. 4 and 5 one can observe the crossover to this regime for $\langle G\rangle < 1$. A more detailed view is supplied in Fig. 7 where apart from the data from Figs. 4 and 5 replotted in $(S-\frac{1}{3}G)$ vs G coordinates new data series obtained for stronger disorder (up to $W=12$) are shown. One can observe that both for the one- and two-dimensional cases the data for various W's and L's follow the same line, giving rise to the conclusion that in both dimensionalities $\langle G\rangle$ is the relevant scaling parameter. This is in accordance with the results derived from RMT. In this approach the increasing wire length leads to the so-called crystallization of transmission eigenvalues λ_n of the transfer matrix ($\mathbf{M}$) which are related to transmission eigenvalues T_n by

$$T_n = \frac{1}{\cosh^2 \lambda_n}. \tag{20}$$

Namely, in this limit ($L \gg \xi_l = N_\perp l$) the eigenvalues $\lambda_n = \langle \lambda_n \rangle + \delta\lambda_n$ with small Gaussian fluctuations $\delta\lambda_n$ around the average $\langle \lambda_n \rangle = nL/\xi_l$, $n=1,2,\ldots$. This is contrary to the diffusive limit $L/l \gg 1$ where it was conjectured that the eigenvalues λ_n have the uniform density[7,15]

$$\rho(\lambda) = \frac{N_\perp l}{L} = \frac{G}{2e^2/h}, \tag{21}$$

with a cutoff at $\lambda \cong L/l$. The transition from a uniform (liquidlike) distribution $\rho(\lambda)$ of Eq. (20) to a crystal-like eigenvalue density was shown to be a function of only two parameters λ and L/l.[15] This means that both G and S are functions of only one parameter, L/l, which can be ruled out. The S vs G relation is unique as we observe in our Figs. 4 and 7. The data in Figs. 5 and 7 show that this conclusion is valid also for the 2D case, which is a less obvious result since RMT in principle works in 1D. The other conclusion is that the transition to strong localization is described by a ''superuniversal'' crossover curve which splits into dimension-dependent branches only when approaching a weak localization limit, $\langle G\rangle \gg 1$.

VI. CONCLUSIONS

In summary a detailed numerical study of shot noise power in disordered phase-coherent one- and two-dimensional conductors has been performed. For the quasi-1D case excellent agreement with the results of RMT has been found in ballistic, metallic, and insulating regimes. For two-dimensional geometry we show that (i) the crossover from ballistic to metallic and from weak to strong localization regimes follows the same relation as for the 1D case and (ii) in the regime of weak localization the shot noise power S exceeds the one-third suppression value by a value of $\delta\tilde{S} = 0.123\,74$, $S = \frac{1}{3}G + \delta\tilde{S}\,2e^2/h$.

ACKNOWLEDGMENTS

This work was supported by the Polish State Committee for Scientific Research (KBN) through Grant No. 8-T11B-05515. The authors express their thanks to T. Dietl for encouraging them to do this work.

[1] W. Schottky, Ann. Phys. (Leipzig) **57**, 541 (1918).
[2] Ya.M. Blanter and M. Büttiker, Phys. Rep. **336**, 1 (2000).
[3] M. Büttiker, Phys. Rev. Lett. **65**, 2901 (1990).
[4] C.W.J. Beenakker and M. Büttiker, Phys. Rev. B **46**, 1889 (1992).
[5] M. Henny, S. Oberholzer, C. Strunk, and C. Schönenberger, Phys. Rev. B **59**, 2871 (1999).
[6] O.N. Dorokhov, Solid State Commun. **51**, 381 (1984).
[7] A.D. Stone, P.A. Mello, K.A. Muttalib, and J.-L. Pichard, in *Mesoscopic Phenomena in Solids*, edited by B.L. Altshuler, P.A. Lee, and R.A. Webb (North-Holland, Amsterdam, 1991), p. 369.
[8] Yu.V. Nazarov, Phys. Rev. Lett. **73**, 134 (1994).
[9] M.J.M. de Jong and C.W.J. Beenakker, Phys. Rev. B **46**, 13 400 (1992).
[10] P.A. Mello, Phys. Rev. Lett. **60**, 1089 (1994).
[11] Yu.V. Nazarov, Phys. Rev. B **52**, 4720 (1995).
[12] S. Datta, *Electronic Transport in Mesoscopic Systems* (Cambridge University Press, Cambridge, England, 1995).
[13] D.S. Fisher and P.A. Lee, Phys. Rev. B **23**, 6851 (1981).
[14] R.C. Liu, P. Eastman, and Y. Yamamoto, Solid State Commun. **102**, 785 (1997).
[15] C.W.J. Beenakker, Rev. Mod. Phys. **69**, 731 (1997).
[16] A.M.S. Macêdo, Phys. Rev. Lett. **79**, 5098 (1997).